THE JOURNAL OF BIOLOGICAL CHEMISTRY Vol. 279, No. 2, Issue of January 9, pp. 1474–1481, 2004

Printed in U.S.A.

Identification of an Expanded Binding Surface on the FADD Death Domain Responsible for Interaction with CD95/Fas*[S]

Received for publication, May 13, 2003, and in revised form, October 22, 2003
Published, JBC Papers in Press, October 22, 2003, DOI 10.1074/jbc.M304996200

Justine M. Hill‡§, Gaku Morisawa§, Tad Kim, Ted Huang, Yu Wei, Yufeng Wei, and Milton H. Werner¶

From the Laboratory of Molecular Biophysics, The Rockefeller University, New York, New York 10021

The initiation of programmed cell death at CD95 (Fas, Apo-1) is achieved by forming a death-inducing signaling complex (DISC) at the cytoplasmic membrane surface. Assembly of the DISC has been proposed to occur via homotypic interactions between the death domain (DD) of FADD and the cytoplasmic domain of CD95. Previous analysis of the FADD/CD95 interaction led to the identification of a putative CD95 binding surface within FADD DD formed by α helices 2 and 3. More detailed analysis of the CD95/FADD DD interaction now demonstrates that a bimodal surface exists in the FADD DD for interaction with CD95. An expansive surface on one side of the domain is composed of elements in α helices 1, 2, 3, 5, and 6. This major surface is common to many proteins harboring this motif, whether or not they are associated with programmed cell death. A secondary surface resides on the opposite face of the domain and involves residues in helices 3 and 4. The major surface is topologically similar to the protein interaction surface identified in *Drosophila* Tube DD and the death effector domain of hamster PEA-15, two physiologically unrelated proteins which interact with structurally unrelated binding partners. These results demonstrate the presence of a structurally conserved surface within the DD which can mediate protein recognition with homo- and heterotypic binding partners, whereas a second surface may be responsible for stabilizing the higher order complex in the DISC.

The subgroup of tumor necrosis factor receptor (TNFR)[1] superfamily members that contain a death domain (DD) within their cytoplasmic region have been termed "death receptors" (1). The receptor DD is the nucleus of an intracellular death-inducing cellular signaling complex (DISC), which forms in response to ligand binding by the receptor. The DISC of CD95 (Fas, Apo-1), one of six TNFRs that initiate cell death, is composed of the activated receptor (2, 3), the adaptor protein FADD (4, 5), and the initiator caspases, caspase-8 (6–8) and caspase-10 (9, 10). A key molecule in this assembly is FADD, which links the death receptor to the caspases, a function attributed to FADD at nearly all death receptors identified to date (1). FADD contains two ~90-amino acid protein interaction modules, an N-terminal death effector domain (DED), and a C-terminal DD, each of which adopts a structurally similar six α-helical bundle (11–13). It has been suggested that the two domains of FADD function independently of each other (4, 5), with the DD responsible for interaction with CD95 and the DED responsible for the subsequent recruitment of caspases into the DISC (11–13).

Despite knowledge of the three-dimensional structures of the DD (12–17) and DED (11, 18) motifs from a variety of proteins, the mechanism of protein recognition by these structurally homologous motifs has not been clearly defined. The crystal structure of *Drosophila* Tube DD bound to the DD from the serine/threonine kinase Pelle demonstrated that the DD motif possessed two distinct and opposing protein interaction surfaces within their folded domains (16). One surface (the "loop surface") is formed principally by an interhelical loop and the adjacent 1–2 turns of α helix found at the junction of helices 1 and 2 and helices 5 and 6, as exemplified in Tube DD (Fig. 1). The second surface, exemplified by Pelle DD, is formed by α helices 3 and 4 and the loop connecting helices 4 and 5, all located on the opposite side of the motif relative to the "loop surface" (Fig. 1). Remarkably, although the DD fold is highly conserved, characterization of the homologous domains found in the cell death proteins FADD (12, 19), CD95 (14), and TRADD (20) all suggested a binding surface for their partners that diverged from Tube and Pelle. Thus, it was conceivable that apoptotic proteins harboring a DD motif might utilize the domain in a unique fashion relative to those proteins which are involved in other signaling pathways, such as Tube and Pelle. Furthermore, the relatively low pairwise sequence identity between DDs seemed consistent with the notion of divergent protein-protein interaction mechanisms for the same overall three-dimensional structure.

We recently demonstrated that the DED of the phosphoprotein enriched in astrocytes, PEA-15, utilizes a Tube-like surface for interaction with its binding partner, the extracellular signal-regulated kinase mitogen-activated protein mitogen-activated protein kinase (Ref. 18; Fig. 1). The topological similarity in the DD and DED motif interactions in these two cases prompted a reexamination of the protein recognition mecha-

* This work was supported in part by Fellowship LT0537 from the Human Frontier Science Program, Grant 997045 from the National Health and Medical Research Council of Australia, the Norman and Rosita Winston Foundation (to J. M. H.), the National Science Foundation, the National Institutes of Health, and Irma T. Hirschl Trust grants (to M. H. W.). The costs of publication of this article were defrayed in part by the payment of page charges. This article must therefore be hereby marked "*advertisement*" in accordance with 18 U.S.C. Section 1734 solely to indicate this fact.

[S] The on-line version of this article (available at http://www.jbc.org) contains additional data.

‡ Present address: Institute of Molecular Bioscience, University of Queensland, Brisbane, QLD 4072, Australia.

§ These authors contributed equally to this work.

¶ A Distinguished Young Scholar of the W. M. Keck Foundation. To whom correspondence should be addressed: Laboratory of Molecular Biophysics, The Rockefeller University, 1230 York Avenue, Box 42, New York, NY 10021. Tel.: 212-327-7221; Fax: 212-327-7222; E-mail: mwerner@portugal.rockefeller.edu.

[1] The abbreviations used are: TNFR, tumor necrosis factor receptor; DD, death domain; DISC, death-inducing cellular signaling complex; GST, glutathione *S*-transferase;HA, hemagglutinin;GFP, green fluorescent protein; HSQC, heteronuclear single quantum coherence; CARD, caspase recruitment domain.

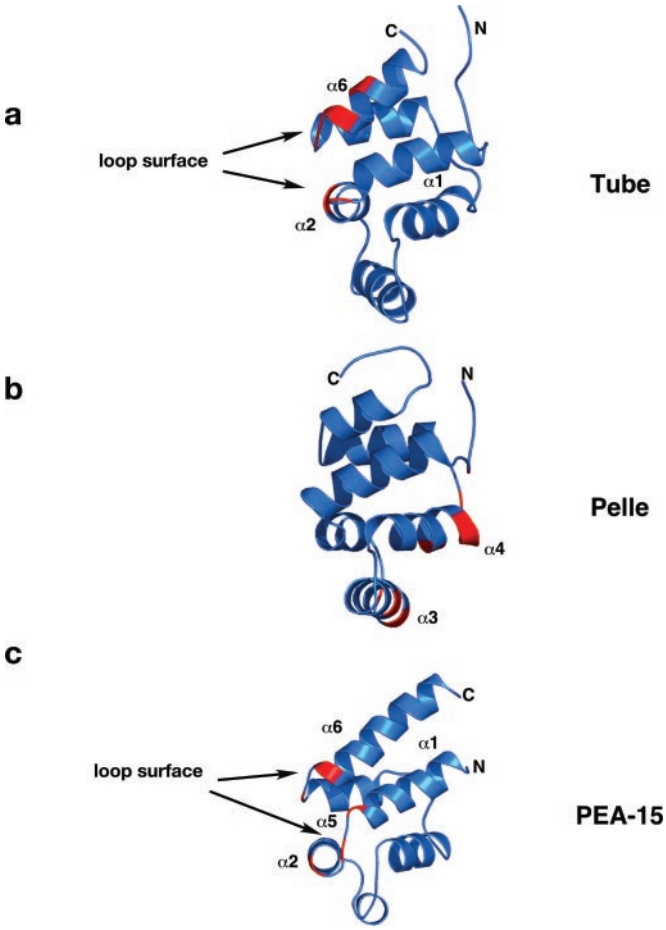

FIG. 1. **Conserved protein-interaction surfaces of death domains and death effector domains.** Backbone representations of the Tube DD (*a*) (16), Pelle DD (*b*) (16), and PEA-15 DD (*c*) (18) are shown in *blue*, with residues important for binding their target proteins highlighted in *red*. The two principle binding surfaces are the loop surface composed of residues in the interhelical loop and adjacent turns of α helix between helices 1 and 2, as well as helices 5 and 6. The second surface resides principally in α helix 4 on the opposite side of the motif relative to the loop surface, as exemplified in Pelle.

nism(s) involving these motifs among apoptotic factors. Characterization of a panel of mutants introduced into the DD of FADD, in the context of the full-length protein, now demonstrates that the FADD DD interaction with the cytoplasmic domain of CD95 is also related to the protein interaction mechanism employed by Tube DD. The loop surface in FADD DD is extended further into α helix 2 and α helix 3 relative to Tube DD. In addition, a small patch of positively charged residues residing in helices 3 and 4, on the opposite face of the domain from the loop surface, also display reduced binding to CD95. Thus, FADD recruitment into the DISC may be bimodal. Mutations across the CD95 interaction surface substantially reduce the relative cell-killing activity of FADD in cell culture, consistent with the reduced affinity of mutant FADD proteins for CD95 in reconstitution experiments. Immunoprecipitation of CD95 DISCs under these conditions demonstrates that reduced cell killing of mutant FADD in culture is caused by a reduced ability of mutant FADD to assemble the CD95 DISC. These results suggest an alternative view from which protein recognition by the DD of cell death-associated proteins may be understood, namely, that the binding surface of a DD for an apoptotic partner is topologically conserved with that of non-apoptotic proteins harboring structurally related motifs. The diversity in protein recognition mechanisms by the DD and DED motifs is thus achieved by the expansion of a core, conserved interaction surface to distinguish functionally diverse binding partners.

MATERIALS AND METHODS

Proteins and DNAs—cDNA of full-length human FADD was inserted into pET-28b (Novagen) and specific amino acid mutations were generated with the QuikChange site-directed mutagenesis kit (Stratagene). Mutants of FADD were constructed in which surface-exposed residues (identified by inspection of the individual domain structures; Refs. 12 and 13) were substantially altered in side chain length and/or charge, while minimizing the likelihood of altering the protein structure. The resulting mutations were confirmed by DNA sequencing. Wild-type and mutant FADDs were expressed *in vitro* using the TNT T7 coupled reticulocyte lysate system (Promega) in the presence of [^{35}S]methionine. The intracellular domain of human CD95 was overexpressed as a GST fusion protein using a pGEX-6P-1 vector (Amersham Biosciences) and batch purified on glutathione agarose beads (Sigma). An enforced trimer of the CD95 cytoplasmic domain was constructed using a trimeric coiled coil (21) fused to residues 178–304 of CD95 in the pQE-30 vector (Qiagen). The overexpressed fusion protein was purified under denaturing conditions using Ni^{2+}-affinity chromatography. Refolding was initiated by dilution of the purified protein into 6 M guanidine hydrochloride (GnHCl), 50 mM Tris-HCl, pH 8.0, 500 mM NaCl, 2 mM dithiothreitol, 5% glycerol (v/v) at a final protein concentration of 0.2–0.4 mg/ml, followed by stepwise dialysis to 2 M GnHCl over 12 h, then 0 M GnHCl over 12 h at 4 °C in the same buffer. The refolded protein was concentrated to 1–2 mg/ml and fractionated by preparative size-exclusion chromatography using Superdex-75. The eluted protein appears as a symmetrical peak and is judged to be homogenously trimeric based on the calibrated elution volume from the column. For immunofluorescence, cell viability, and co-immunoprecipitation experiments, human FADD was inserted into pcDNA 3.0 (Invitrogen) with a hemagglutinin (HA) tag at the C terminus.

In Vitro Protein Interaction Assay—GST-CD95 intracellular domain was mixed with wild-type FADD or mutant FADD in a 150 μl solution containing 50 mM HEPES-KOH, pH 7.4, 50 mM NaCl, 0.1% Nonidet P-40, 5 mM EDTA, and 10% glycerol (w/v). Binding was conducted at 4 °C for 2 h. The bound complex was washed three times with 500 μl of the same buffer and the proteins eluted with SDS-PAGE loading dye, separated by 16% Tricine SDS-PAGE, and visualized by phosphorimaging. For trimeric CD95, the protein was immobilized on Ni^{2+}-agarose, and pull-down experiments with FADD were performed in a 150 μl solution containing 50 mM HEPES-KOH, pH 7.4, 50 mM NaCl, 0.1% Nonidet P-40, 10% glycerol, and 70 mM imidazole as described above.

Cell Viability Assay—Cell viability was measured in triplicate between 12 and 24 h after transfection with pcDNA 3.0 harboring either wild-type FADD or mutant FADD. 200 ng of FADD plasmid DNA was co-transfected with 20 ng of plasmid harboring GFP into MCF7-Fas cells (22) and incubated for 6 h; apoptosis was induced by the addition of an aggregating anti-Fas antibody (CH11, Upstate Biotechnology). Cell morphology was followed by GFP fluorescence, and chromatin condensation was followed by Hoechst staining of cells. Approximately 100 GFP-positive cells were counted in triplicate to determine the relative rate and extent of cell death in the presence or absence of anti-CD95 treatment.

Immunoprecipitation—For co-immunoprecipitation with anti-Fas, MCF7-Fas cells were transfected with 4 μg of either wild-type FADD or mutant FADD. For DISC assembly, anti-CD95 antibody (APO-1–3, Kamiya Biomedical) was added to the media 6 h after transfection and incubated at 37 °C for 5 min. Cells were lysed on ice with immunoprecipitation binding buffer (30 mM Tris-HCl, pH 7.5, 150 mM NaCl, 2 mM EDTA, 1 mM phenylmethylsulfonyl fluoride, protease inhibitors mixture (Roche Applied Science), 1% Triton X-100, and 10% glycerol) for 30 min. The lysate was spun at 14,000 $\times$ *g* for 15 min. Protein A magnetic beads (New England Biolabs) were added to the lysate and incubated for another 3 h. Beads were washed three times with IP buffer. After SDS-PAGE, the proteins were blotted onto nitrocellulose membrane for immunodetection and probed with anti-HA antibody (3F10, Roche Applied Science). As a negative control, MCF7-Fas cells transfected with a vector expressing wild-type FADD-HA were lysed 6 h after transfection, and anti-CD95 was added for 5 min at the end of the lysis period but prior to immunoprecipitation with protein A magnetic beads.

NMR Spectroscopy—^{1}H-^{15}N heteronuclear single quantum coherence (HSQC) spectra were collected for the individual domains of FADD containing single point mutants defective for CD95 binding. FADD DD (residues 89–183) was cloned into pQE-9 (Qiagen), which produced the recombinant protein domain with a His_6 sequence at the N terminus.

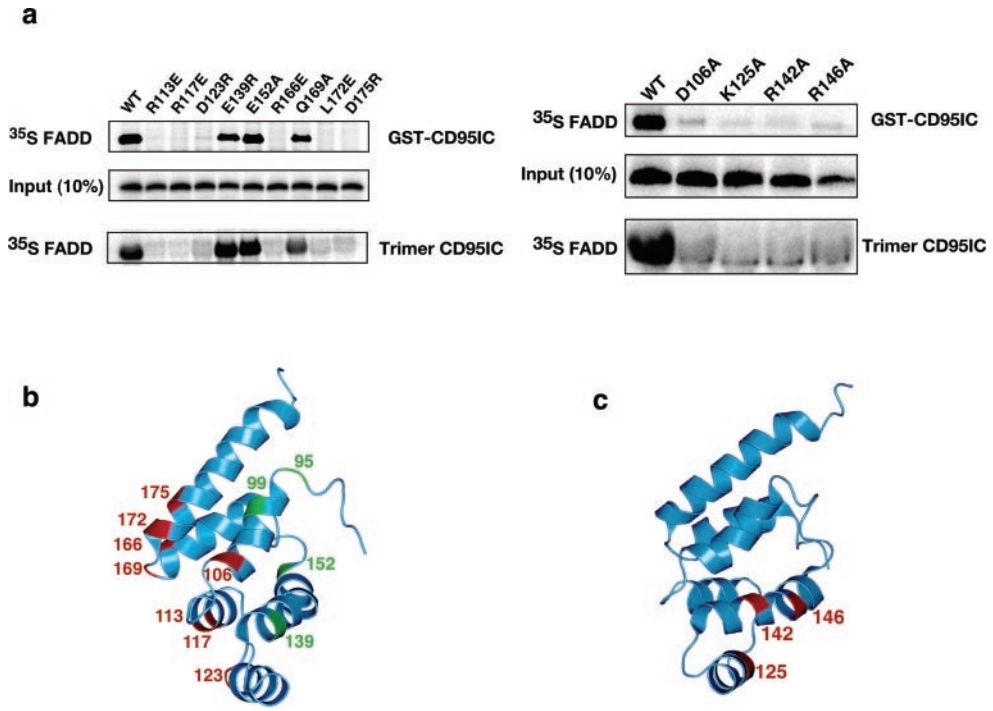

FIG. 2. **Identification of the FADD DD binding surface for CD95.** *a*, site-directed mutagenesis of surface-exposed residues in FADD DD (in the context of the full-length protein) reveals residues within α helices 1 (D106A), 2 (R113E, R117E), 3 (D123R), 5 (R166E), and 6 (L172E, D175R), as well as the helix 5–6 loop (Q169A) that contributes to CD95 binding. In addition to those shown, mutants in helix 1 (E95R and A99E) and helix 4 (E139R, E152A) were also tested in a GST pull-down and found to be similar to wild-type. The relative binding efficiency of FADD or FADD mutant to a GST-CD95 intracellular domain fusion protein (GST-CD95IC) is nearly identical to that of an activated CD95 receptor mimic (trimer CD95IC) created by fusing the intracellular domain of CD95 to a trimeric coiled-coil (21). These results suggest that domain-to-domain interaction between FADD and CD95 is not influenced by the oligomeric state of the receptor. *b*, binding-defective DD mutants mapped onto the three-dimensional structure of FADD DD (13). All of these CD95 binding-deficient mutants (*red*) reside on one face of the domain. Those mutants that did not affect CD95 binding in a GST pull-down assay are colored *green*. *c*, additional binding-defective mutants from *a*, which reside on the opposite face of the FADD DD relative to those in *b*, are highlighted in *red*. This view of the FADD DD is rotated 60° clockwise around the *y* axis relative to the view in *b*.

^{15}N-labeled proteins were produced on a small scale in shake flasks and purified with Ni^{2+}-affinity chromatography. NMR samples contained ~0.3 mM protein in 50 mM potassium phosphate buffer, pH 6.2, 150 mM NaCl, 1 mM dithiothreitol, and 50 μM NaN_3 for FADD DD. Two-dimensional ^{1}H-^{15}N HSQC spectra of the mutant proteins were compared with those of the wild-type DD to establish that the mutant proteins possessed the same overall three-dimensional structure.

RESULTS

Identification of the FADD DD Binding Surface for CD95—To elucidate the mechanism of FADD recruitment to CD95, site-directed mutagenesis was used to identify functionally important residues within the FADD DD that are involved in binding to the receptor cytoplasmic domain. Mutants were constructed in which surface-exposed residues were substantially altered in side-chain length and/or charge while minimizing the likelihood of altering the protein structure. Characterization of these mutants by GST-pull-down assay with the intracellular domain of CD95 (GST-CD95IC) revealed a binding surface for CD95 that traverses all six α helices of the FADD DD (Fig. 2 and Table I). Residues within α helices 1 (D106R), 2 (R113E, R117E), 3 (D123R), 5 (R166E), and 6 (L172E, D175R) as well as the helix 5–6 loop (Q169A) of FADD DD all contribute to CD95 binding on one face of the domain (Fig. 2, *a–c*). An additional set of mutants in helices 3 (K125A) and 4 (R142A/E, R146A) were also shown to be defective for CD95 interaction in a GST pull-down assay.

Activated CD95 in cells is most likely trimeric; thus, it may be reasonably questioned whether GST-CD95IC immobilized on agarose beads appropriately represents the cellular state of the activated receptor. To mimic the trimeric receptor, an "artificial receptor" was created by fusing CD95IC C-terminal to a peptide known to form a trimeric coiled-coil (21). The trimeric "artificial" receptor was purified to homogeneity by size-exclusion chromatography, which ensured that a well defined trimer of the CD95 cytoplasmic domain had been created. This artificial receptor was then used to probe the FADD DD mutants using an Ni^{2+}-affinity bead pull-down assay. FADD DD mutants that failed to bind GST-CD95 also failed to bind trimeric

TABLE I
Mutagenesis of FADD within the death domain

Mutation	Activity[a]	Fold[b]
E95R	++[c]	NT
A99E	++	NT
D106A	−	Native
R113E	−	Native
R117E	−	Native
D123R	−	Native
K125A	−	Native
E139R	++	NT
R142A	−	Native
R142E	−	NT
R146A	−	Native
E152A	++	NT
R166E	−	Native
Q169A	+	Native
L172E	−	Native
D175R	−	Native

[a] Activity determined by quantitation of band intensity in a GST-pulldown assay relative to a GST-only control.
[b] Fold determined by similarity in peak pattern of ^{15}N-^{1}H HSOC spectra of N-terminally hexahistidine-tagged FADD DD (residues 89–183) mutant compared to wildtype.
[c] ++, ≥50% of wildtype; +, 10–50% wildtype; −, ≤10% wildtype; NT, not tested.

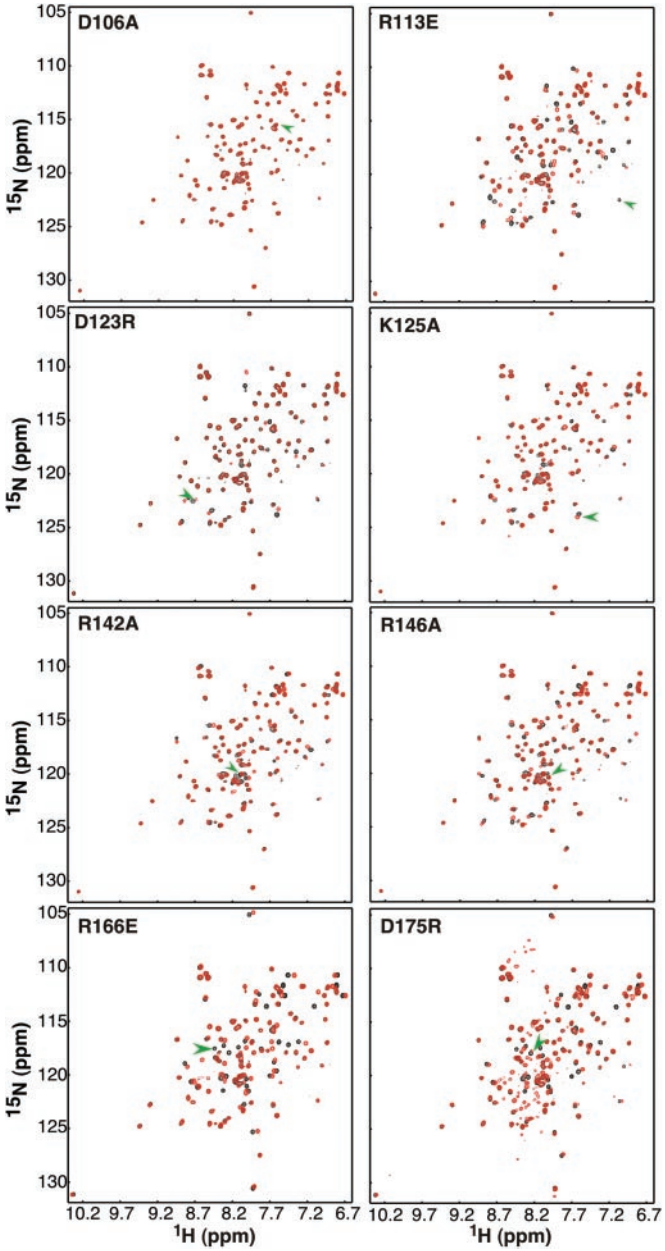

FIG. 3. **Site-directed mutants of FADD DD are structurally similar to the wild-type protein.** ^{15}N-^{1}H HSQC spectra of wild type (*black*) and mutant FADD DD (*red*) are nearly identical for D106A, R113E, D123R, K125A, R142A, R146A, R166E, and D175R. NMR spectra of the wild-type and mutant DDs were collected at 25 °C in 50 mM potassium phosphate buffer, pH 6.2, 150 mM NaCl, and 1 mM dithiothreitol. Although there are a few shifted peaks in each mutant spectrum shown, these are most likely the consequence of the change in a locally charged surface. All of the mutant spectra (*red*) are well dispersed and display an overall pattern of peaks consistent with the fold of the wild-type protein domain (*black*). The peak corresponding to the residue mutated in the wild-type protein is indicated by the *green arrow*.

CD95 (Fig. 2*a*), displaying a nearly identical binding profile for trimeric CD95 as that observed for the GST-fusion protein.

FADD DD Mutants Retain Their Structural Integrity—Because the mutation strategy substantially altered the physical property of the native amino acid at any mutated position, each mutant protein was analyzed by ^{15}N-^{1}H NMR correlation spectroscopy to determine whether the protein structure had been altered by the mutation. The pattern of NMR crosspeaks in the mutant protein NMR spectra were similar to that of the native DD, with only minor changes in the peak pattern observed in each case (Fig. 3). These data demonstrate that the CD95 binding-defective mutants of FADD most likely possessed a native-like three-dimensional fold. Thus, the loss in binding by any FADD mutant in a pull-down experiment was due to a reduction in binding affinity for CD95 as a consequence of the mutation.

Functional Analysis of FADD DD Mutant Proteins in MCF7-Fas Cells—To confirm the physiological relevance of reduced FADD binding to CD95 in a pull-down assay, the FADD DD mutants that exhibited reduced CD95 association *in vitro* were expressed in MCF7-Fas cells and tested for their ability to induce apoptosis in cell culture (Fig. 4). A plasmid expressing FADD or FADD mutant fused to an HA tag was transfected into MCF7-Fas cells, and the cells were subsequently stimulated at the CD95 receptor with an aggregating antibody known to activate the receptor. The time course of cell death was then followed, as determined by characteristic changes in cell morphology and chromatin condensation (Fig. 4). As a control experiment, the effect of FADD overexpression in the absence of receptor stimulation was followed under identical conditions. In unstimulated cells, the rate and extent of cell death in the presence of overexpressed FADD were quite modest during the first 24 h after transfection and mirror the effect of transfection with the pcDNA vector itself (Fig. 4, *a* and *b*). Thus, FADD overexpression, at the level employed in this study, is inefficient at inducing cell death in the absence of an apoptotic stimulus of these cells. By contrast, stimulation of CD95 after transfection with a FADD expression vector resulted in the death of ≥80% of the culture within 24 h (Fig. 4, *c* and *d*). The mutant FADD proteins display a differential ability to support stimulated cell death. D106A, R113E, and D175R are among the most deficient mutants and fail to display a pull-down with either GST-CD95IC or trimer CD95IC. Q169A, on the other hand, is similar to wild type in its relative cell-killing ability, which mirrors the minor reduction of Q169A binding seen in the pull-down assays. For those residues forming a small positive patch on a secondary surface, the correlation of the pull-down and cell viability data is less clear. Both K125A and R142A fail to show a pull-down response, but K125A is quite similar to Q169A in terms of its effect on cell killing. For this reason, it is possible that the positive patch formed by Lys125, Arg142, and Arg146 may play a secondary role in the assembly of the signaling complex. Clearly the effect of the mutants is more graded in cultured cells (Fig. 4*c*) relative to the all or nothing response observed by the *in vitro* pull-down experiment (Fig. 2*a*). This is most likely caused by the extensive washing of the FADD-loaded CD95IC beads in the pull-down, which could wash away all but the most able CD95 binding mutants of FADD. The relative cell-killing ability of the overexpressed FADD proteins in cell culture was not a consequence of differential expression of FADD or FADD mutants. Western blot analysis of cell extracts (Fig. 4*a*, *Inset*) demonstrates that the wild-type and mutant proteins were expressed at nearly equal levels in these cells.

To further demonstrate the role of FADD DD residues in CD95 interaction, MCF7-Fas cells were activated in the presence of overexpressed wild-type or mutant FADD, and the DISCs were subsequently isolated by anti-CD95 immunoprecipitation (DISC IP), while the majority of the cells were still alive (Fig. 5). The precipitated proteins were then visualized by anti-HA Western blot to view the relative levels of wild-type or mutant FADD in the CD95 DISC (Fig. 5). DISC IP confirmed the results seen *in vitro*, namely, that the mutant FADD proteins inefficiently associate with CD95. A control experiment in which anti-CD95 was added after lysis of the cells failed to immunoprecipitate FADD, indicating that the reduced associ-

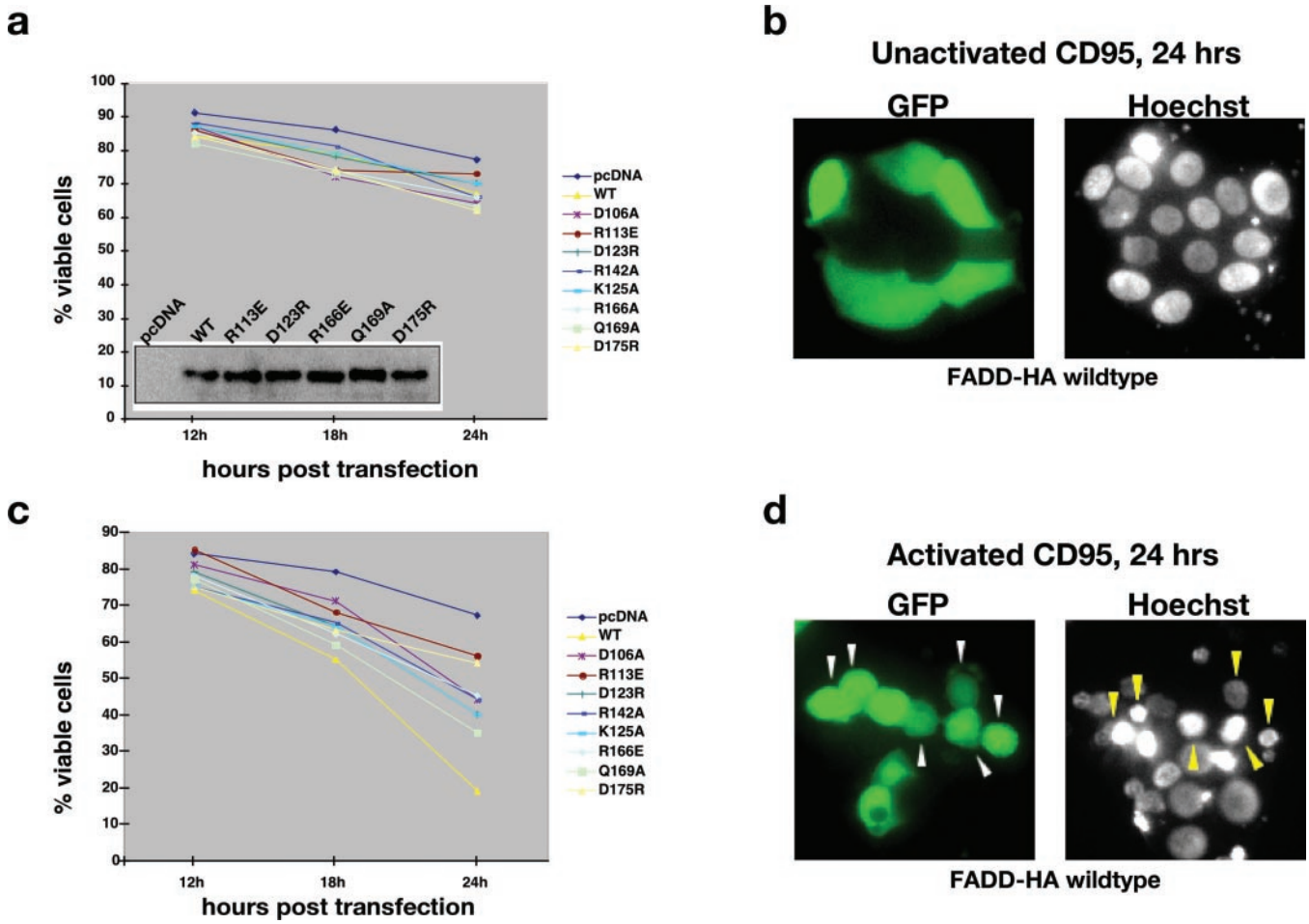

FIG. 4. **CD95 binding defective mutants of FADD display reduced apoptosis in MCF7-Fas cells.** The rate and extent of apoptosis were followed by analysis of cell morphology and chromatin condensation at the indicated times. Approximately 100 cells were counted for each mutant at each time point in triplicate. Standard deviations have been excluded for clarity, but they vary between 3–9%. *a*, unstimulated MCF7-Fas cells were transfected with wild-type or mutant full-length FADD harboring a single mutation at the indicated position in the FADD DD. Transfected cells were identified by GFP fluorescence and counted based on the morphology of the cell and the appearance of the nuclei after Hoechst staining. In the absence of a stimulus, the rate and extent of cell death induced by overexpression of FADD are essentially equivalent to that of transfection with the pcDNA vector control, indicating that the overexpression of FADD or FADD mutant is inefficient at inducing apoptosis in the absence of receptor stimulus. *Inset,* an anti-hemagglutinin Western blot of the expression level of FADD or FADD mutant in unstimulated cells, demonstrating that the observed effects are not the consequence of differential expression of the proteins. Actin was used as a loading control (not shown). D106A, K125A, and R142A all expressed at levels approximately equal to those of wild type (not shown). *b*, an example of the scoring of cell counts is shown for transfected, wild-type FADD with a C-terminal hemagglutinin tag (*FADD-HA*) at the 24-h time point. Both cell morphology and Hoechst staining demonstrate that the cells are essentially unaffected by overexpression of FADD in the absence of CD95 activation. *c*, in cells stimulated at the CD95 receptor by an aggregating antibody (see "Materials and Methods"), rates of cell death are impaired for mutant FADD which displayed reduced association with GST-CD95 or a trimeric CD95-receptor mimic in a pull-down assay (Fig. 2*a*). The relative efficiency of the FADD mutants to induce apoptosis in cell culture mirrors the relative ability of mutant FADD to associate with CD95 in a pull-down assay. Standard deviations have been excluded for clarity, but they vary between 3–9% (see "Supplemental Material"). *d*, representative scoring of cell death after 24 h overexpression of wild-type FADD-HA in receptor-stimulated MCF7-Fas cells. Both the rounded cell morphology and Hoechst staining of shrunken nuclei (indicated by *arrowheads*) demonstrate that FADD-HA overexpression efficiently kills the cells by apoptosis after receptor stimulation.

ation of mutant FADD into the DISC was specific to complex assembly. The correlation between the binding affinity of the FADD mutants both *in vitro* and *in vivo* and the pro-apoptotic potential of these mutants in MCF7-Fas cells confirms that the CD95-binding surface was identified in the pull-down assays.

DISCUSSION

The death motif superfamily, composed of the DD, DED, and caspase recruitment domain (CARD), are the primary mediators of protein-protein interactions required for the transmission and regulation of apoptotic signals (23). Commensurate with the importance of elucidating the molecular basis and specificity of death motif interactions, numerous structural and mutagenesis studies of individual domains have been undertaken (11–15, 17–20, 24, 25), and x-ray crystal structures have been determined for heterodimer complexes formed by the CARDs of Apaf-1 and procaspase-9 (26) and the DDs of *Drosophila* Tube and Pelle (16). However, no common protein interaction surfaces have been revealed from these studies as the residues that form the interface are dramatically different between these two heterodimer structures; they also differ from the surfaces suggested by mutagenesis to mediate other death motif interactions.

In this study, functional characterization of FADD DD mutants has revealed that an extensive surface spanning elements in all six α helices in the domain is required for CD95 interaction. Pull-down assays using either GST-CD95IC or a trimeric-receptor mimic demonstrate that this extended surface is responsible for the association of FADD DD with CD95 (Fig. 2). Mutants that demonstrated reduced binding efficiency in pull-down assays were deficient at supporting apoptosis and displayed reduced recruitment into the CD95 DISC in MCF7-Fas cells. To minimize the potential interference from endoge-

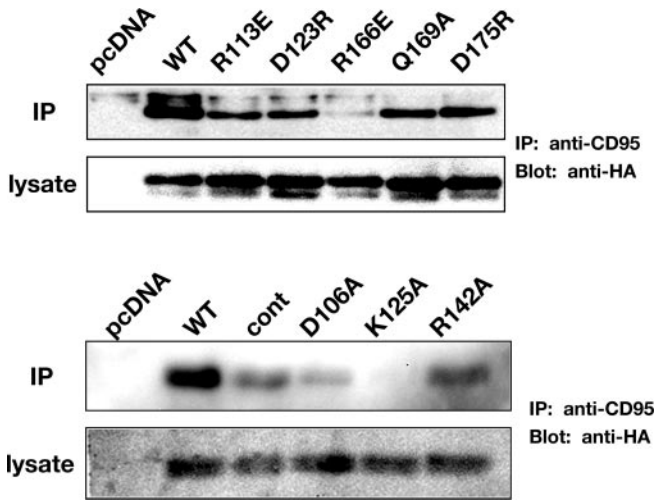

FIG. 5. **Immunoprecipitation of mutant CD95 DISCs demonstrates that mutant FADD inefficiently associates with CD95 *in vivo*.** Anti-CD95 immunoprecipitation was initiated 6 h after transfection of MCF7-Fas cells with an expression plasmid for FADD or FADD mutant. Cultured cells were stimulated for 5 min with anti-CD95 followed by immunoprecipitation, as described under "Materials and Methods." The precipitated DISCs were then probed with an anti-HA antibody to visualize the wild-type or mutant-overexpressed FADD associated with the activated receptor. The time point of immunoprecipitation was chosen such that ≥90% of the cells in culture were alive. The reduced association of the mutant FADDs relative to wild type demonstrates that the reduced cell-killing ability of mutant FADD (Fig. 4) is a consequence of inefficient assembly of activated receptor DISCs. The *cont* lane indicates the addition of anti-CD95 after cell lysis of unstimulated cells for 5 min before immunoprecipitation. As expected, very little FADD-HA is immunoprecipitated by anti-CD95 in this control experiment, as no DISCs would have been present.

nous FADD in these experiments, MCF7-Fas cells were stimulated 6 h after transfection. At this time, the overexpressed FADD protein was clearly discernable by immunofluorescence microscopy, indicating that the level of overexpressed protein greatly exceeds that of the endogenous FADD and should compete effectively with the endogenous protein for CD95 binding sites. A potential issue in this approach is the effect of FADD overexpression on the analysis of apoptotic signaling in cell culture. If overexpressed FADD can kill the cells by a CD95-independent mechanism, then our measurement of relative cell-killing ability would not report on the efficiency of CD95 DISC formation. However, it was observed that MCF7-Fas cells are insensitive to FADD overexpression unless the receptor is stimulated. The morphologic changes observed in these cells upon receptor stimulation (Fig. 4) are consistent with previous reports (see, for example, Ref. 27). Our results contrast an earlier observation in which overexpression of FADD in CrmA-modified MCF7 cells induced morphologic changes consistent with apoptosis in the absence of a receptor stimulus (5). We can only presume that the CrmA-modified cells contained other uncharacterized defects, making these cells highly sensitive to overexpression of FADD. Alternatively, FADD aggregation may have activated caspases-8 and -10 inside the CrmA-modified cells as a consequence of the 5-fold higher level of plasmid used for transfection of the CrmA-modified cells relative to that employed in Fig. 4. Aggregation and subsequent activation of DISC components as a consequence of very high levels of overexpression is well known to induce cell death (28). Given that the overexpressed proteins in this report did not induce apoptosis in the absence of a stimulus and that the behavior of these mutants in cell culture approximately correlates with the behavior of wild-type and mutant FADD in reconstitution experiments, it is reasonable to assume that overexpression in this instance did not significantly influence the identification of the FADD DD binding surface.

Site-directed mutagenesis of the DDs of FADD (12, 19), CD95 (14), TNFR1 (25), and the TNFR1-associated death domain protein (20) previously implicated α helices 2 and 3 in the mutual interaction of receptor DD with effector DD. These observations were contrasted by the interaction mechanism observed in the crystal structure of a DD complex formed between *Drosophila* Tube and Pelle (16), in which α helices 2 and 6 and the helix 5–6 loop of Tube DD interacted with α helices 3 and 4 of Pelle DD. The disparity in the apparent interaction mechanism of CD95/FADD *versus* Tube/Pelle suggested that the DD may be a promiscuous protein-protein interaction module with multiple potential sites for engaging its binding partners (16, 23). In contrast to this hypothesis, we have shown that the CD95 binding surface within the DD of FADD extends beyond α helices 2 and 3 and is topologically similar to the Pelle-interaction surface of Tube DD (Fig. 6). FADD DD engages CD95 with the loop surface first identified in Tube DD but extends this surface into helices 2 and 3 on the same side of the motif. Similar regions within the two DEDs of MC159, a viral caspase-8 inhibitory protein, have also been implicated in the ability of MC159 to engage its binding partners (29). The relationship between the protein interaction surfaces suggested for the Fas/FADD interaction and the Tube/Pelle interaction is not limited to the interaction between the DD and a partner harboring a homologous motif. Heterologous binding partners for the DED can also follow the Tube/Pelle paradigm, exemplified by the interaction between the phosphoprotein enriched in astrocytes, PEA-15, and extracellular signal-regulated kinase mitogen-activated protein kinase (18). Remarkably, PEA-15 DED employs a Tube-like surface to engage a binding partner with neither sequence nor structural similarity to a DD or DED motif (18). The observation of topologically similar binding surfaces in the FADD DD, the DEDs of MC159, PEA-15 DED, and Tube DD argues strongly that protein-protein interactions mediated by the DD or DED motif likely occur by a common mechanism.

All three members of the death motif superfamily (DD, DED, and CARD) possess a similar three-dimensional structure with a common hydrophobic core (30). The DD and DED can be distinguished from one another on the basis of their amino acid sequences, but functionally they appear to be quite similar (Fig. 6). The DED of PEA-15 (18) and the DD of FADD use a topologically conserved surface to interact with their respective binding partners (Fig. 6*a*). However, the x-ray structure of the Apaf-1/procaspase-9 CARD complex (26) revealed that the CARD may function differently from DD/DED because of the presence of a severely kinked helix 1. Procaspase-9 employs the kink in helix 1, along with helix 4, to interact with residues in helices 2 and 3 of Apaf-1 (Ref. 26; Fig. 6*b*). This arrangement of CARD-CARD interactions diverges from the DD-DD interactions in Tube/Pelle and is inconsistent with the view of the PEA-15 DED (12, 18, 19, and this study; Fig. 6*b*). FADD DD appears to follow the Tube/Pelle paradigm, with an extension of the loop surface into helices 2 and 3 on the same face of the domain. The inclusion of the loop surface as part of the FADD DD interaction surface for CD95 suggests that a CD95/FADD complex will most likely form by a Tube/Pelle-like mechanism at the level of domain-to-domain recognition. This viewpoint is supported by structural and mutagenesis data for homotypic (Refs. 12 and 19, and this study) and heterotypic (18) interactions involving the DD or DED. However, the interaction of FADD with CD95 in the DISC is likely to be more complex than one suggested by consideration of domain-to-domain interac-

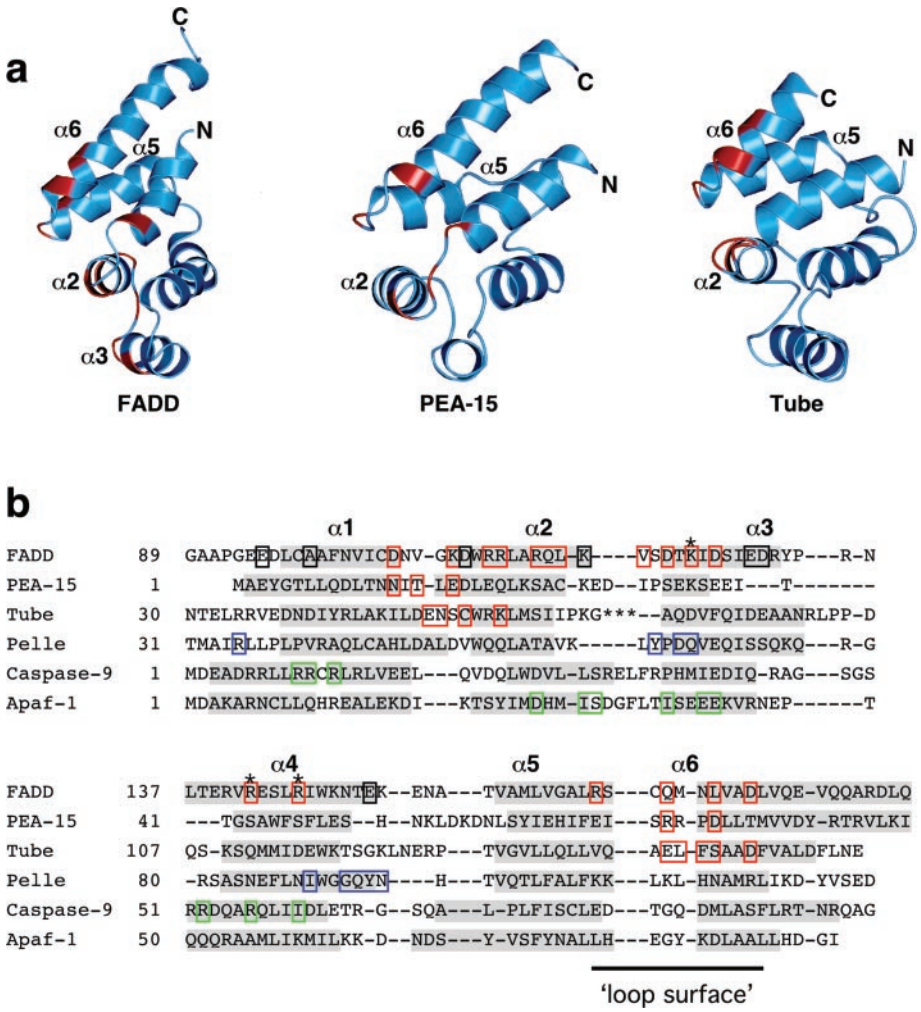

FIG. 6. **Conservation of protein-interaction surfaces for the death domain and death effector domain.** *a*, backbone representations (*blue*) of the three-dimensional structures of FADD DD (12–13), PEA-15 DED (18), and Tube DD (16,) with the residues implicated in forming the protein-interaction surface highlighted in *red*. The two-helix insert in Tube DD relative to the others has been excluded for clarity (16). For PEA-15 DED and Tube DD, the contact surface for their respective binding partners involves nearly identical segments of the three-dimensional structure. FADD DD shares many of the elements of its interaction surface with PEA-15 DED and Tube DD but extends this surface into helices 2 and 3 on the same side of the domain. *b*, structure-based sequence alignment of the FADD DD, PEA-15 DED, Tube DD, Pelle DD, Apaf-1 CARD, and procaspase-9 CARD. The alignment was performed by a pair-wise structure-based alignment using DALI, in which each protein was fit to FADD DD (32). The α-helical segments in each protein domain are shaded *gray*. The residues forming the binding surface observed structurally (16, 26) or inferred by mutagenesis (12, 16, 18, 19, and this study) are boxed in *red*. For FADD DD, PEA-15 DED, and Tube DD, nearly the same regions of each domain are implicated in protein-protein interaction, with the greatest degree of alignment in the portion of the loop surface at helices 5 and 6 as first identified in Tube DD (16). For Pelle DD and the CARDs of Apaf-1 and procaspase-9, the binding surfaces are divergent. Although there is extensive overlap in structurally aligned positions of helices 2 and 3 in FADD DD and Apaf-1 CARD, Apaf-1 lacks the loop surface between helices 5 and 6. It is this loop surface which appears to distinguish Apaf-1/procaspase-9 from Tube/Pelle modes based on these alignments. Three additional mutants of FADD DD which suggest a juxtaposition of the Tube/Pelle and Apaf-1/procaspase-9 modes are *highlighted*, with *asterisks* above a *red box* (see text).

tions alone. Structurally homologous residues in helices 2 and 3 of FADD DD and Apaf-1 CARD are also apparently involved in the interaction with a binding partner in each case (Fig. 6*b*). The same can be said for residues in helix 4 (*i.e.* Arg142 and Arg146) of FADD DD and caspase-9 CARD (Fig. 6*b*). Thus, FADD DD may engage CD95 with a hybrid set of interactions composed of Tube/Pelle and Apaf-1/procaspase-9 modes. One plausible hypothesis may be that Tube/Pelle-like interactions are used for domain-to-domain recognition, and CARD-like interactions help to establish the higher order complex. An intriguing model of the CD95/FADD complex (31) suggests that the DISC is assembled as a 3:3 complex of FADD and CD95 in which the Tube/Pelle and Apaf-1/procaspase-9 modes are juxtaposed, forming Tube/Pelle and Apaf-1/procaspase-9-like interfaces to assemble a higher order complex. The mutants in FADD DD at positions 125, 142, and 146 would seem to support a juxtaposition of these two binding modes in the DISC. Determination of the stoichiometry of these proteins in the complex will be required to further elaborate this model of DISC assembly.

Acknowledgments—We thank Vishva Dixit, Michael Lenardo, and Marcus Peter for cDNAs of human CD95, FADD, and caspase-8, and Marcus Peter for MCF7-Fas cells, antibodies, and many useful discussions.

REFERENCES

1. Ashkenazi, A., and Dixit, V. M. (1998) *Science* **281,** 1305–1308
2. Itoh, N., Yonehara, S., Ishii, A., Yonehara, M., Mizushima, S., Sameshima, M., Hase, A., Seto, Y., and Nagata, S. (1991) *Cell* **66,** 233–243
3. Oehm, A., Behrmann, I., Falk, W., Pawlita, M., Maier, G., Klas, C., Li-Weber, M., Richards, S., Dhein, J., Trauth, B. C., Ponsting, H., and Krammer, P. H. (1992) *J. Biol. Chem.* **267,** 10709–10715
4. Boldin, M. P., Varfolomeev, E. E., Pancer, Z., Mett, I. L., Camonis, J. H., and Wallach, D. (1995) *J. Biol. Chem.* **270,** 7795–7798
5. Chinnaiyan, A. M., O'Rourke, K., Tewari, M., and Dixit, V. M. (1995) *Cell* **81,** 505–512
6. Boldin, M. P., Goncharov, T. M., Goltsev, Y. V., and Wallach, D. (1996) *Cell* **85,**

803–815
7. Muzio, M., Chinnaiyan, A. M., Kischkel, F. C., O'Rourke, K., Shevchenko, A., Ni, J., Scaffidi, C., Bretz, J. D., Zhang, M., Gentz, R., Mann, M., Krammer, P. H., Peter, M. E., and Dixit, V. M. (1996) *Cell* **85,** 817–827
8. Medema, J. P., Scaffidi, C., Kischkel, F. C., Shevchenko, A., Mann, M., Krammer, P. H., and Peter, M. E. (1997) *EMBO J.* **16,** 2794–2804
9. Wang, J., Chun, H. J., Wong, W., Spencer, D. M., and Lenardo, M. J. (2001) *Proc. Natl. Acad. Sci. U. S. A.* **98,** 13884–13888
10. Kischkel, F. C., Lawrence, D. A., Tinel, A., LeBlanc, H., Virmani, A., Schow, P., Gazdar, A., Blenis, J., Arnott, D., and Ashkenazi, A. (2001) *J. Biol. Chem.* **276,** 46639–46646
11. Eberstadt, M., Huang, B., Chen, Z., Meadows, R. P., Ng, S. C., Zheng, L., Lenardo, M. J., and Fesik, S. W. (1998) *Nature* **392,** 941–945
12. Jeong, E. J., Bang, S., Lee, T. H., Park, Y. I., Sim, W. S., and Kim, K. S. (1999) *J. Biol. Chem.* **274,** 16337–16342
13. Berglund, H., Olerenshaw, D., Sankar, A., Federwisch, M., McDonald, N. Q., and Driscoll, P. C. (2000) *J. Mol. Biol.* **302,** 171–188
14. Huang, B., Eberstadt, M., Olejniczak, E. T., Meadows, R. P., and Fesik, S. W. (1996) *Nature* **384,** 638–641
15. Liepnish, E., Ilag, I. L., Otting, G., and Ibañez, C. F. (1997) *EMBO J.* **16,** 4999–5005
16. Xiao, T., Towb, P., Wasserman, S. A., and Sprang, S. R. (1999) *Cell* **99,** 545–555
17. Sukits, S. F., Lin, L.-L., Hsu, S., Malakian, K., Powers, R., and Xu, G-Y. (2001) *J. Mol. Biol.* **310,** 895–906
18. Hill, J. M., Vaidyanathan, H., Ramos, J. W., Ginsberg, M. H., and Werner, M. H. (2002) *EMBO J.* **21,** 6494–6504
19. Bang, S.-H., Jeong, E.-J., Kim, I.-K., Jung, Y.-K., and Kim, K.-S. (2000) *J. Biol. Chem.* **275,** 36217–36222
20. Park, A., and Baichwal, V. R. (1996) *J. Biol. Chem.* **271,** 9858–9862
21. Harbury, P. B., Alber, T., and Kim, P. S. (1994) *Nature* **371,** 80–83
22. Jaattela, M., Benedict, M., Tewari, M., Shayman, J. A., and Dixit, V. M. (1995) *Oncogene* **10,** 2297–2305
23. Fesik, S. W. (2000) *Cell* **103,** 273–282
24. Tartaglia, L. A., Ayres, T. M., Wong, G. H., and Goeddel, D. V. (1993) *Cell* **74,** 845–853
25. Telliez, J. B., Xu, G. Y., Woronicz, J. D., Hsu, S., Wu, J. L., Lin, L., Sukits, S. F., Powers, R., and Lin, L. L. (2000) *J. Mol. Biol.* **300,** 1323–1333
26. Qin, H., Srinivasula, S. M., Wu, G., Fernandes-Alnemri, T., Alnemri, E. S., and Shi, Y. (1999) *Nature* **399,** 549–557
27. Scaffidi, C., Fulda, S., Srinivasan, A., Friesen, C., Li, F., Tomaselli, K. J., Debatin, K.-M., Krammer, P. H., and Peter, M. E. (1998) *EMBO J.* **17,** 1675–1687
28. Siegel, R. M., Martin, D. A., Zheng, L., Ng, S. Y., Bertin, J., Cohen, J., and Lenardo, M. J. (1998) *J. Cell Biol.* **141,** 1243–1253
29. Garvey, T. L., Bertin, J., Siegel, R. M., Wang, G. H., Lenardo, M. J., and Cohen, J. I. (2002) *J. Virol.* **76,** 697–706
30. Vaughn, D. E., Rodriguez, J., Lazebnik, Y., and Joshua-Tor, L. (1999) *J. Biol. Chem.* **293,** 439–447
31. Weber, C. H., and Vincenz, C. (2001) *FEBS Lett.* **492,** 171–176
32. Holm, L., and Sander, C. (1993) *J. Mol. Biol.* **233,** 123–138

Supplementary Material

Figure A: Viability of cultured cells 24 hr following expression of FADD or FADD mutant in CD95-stimulated MCF7-Fas cells. The histogram illustrates the % viable cells as determined by cell morphology and Hoechst staining of nuclei 24 hr after transfection with an expression plasmid for FADD or FADD mutant and stimulation with anti-CD95 as described in *Methods*. Error bars represent one standard deviation from triplicate counts of approximately 100 cells each.

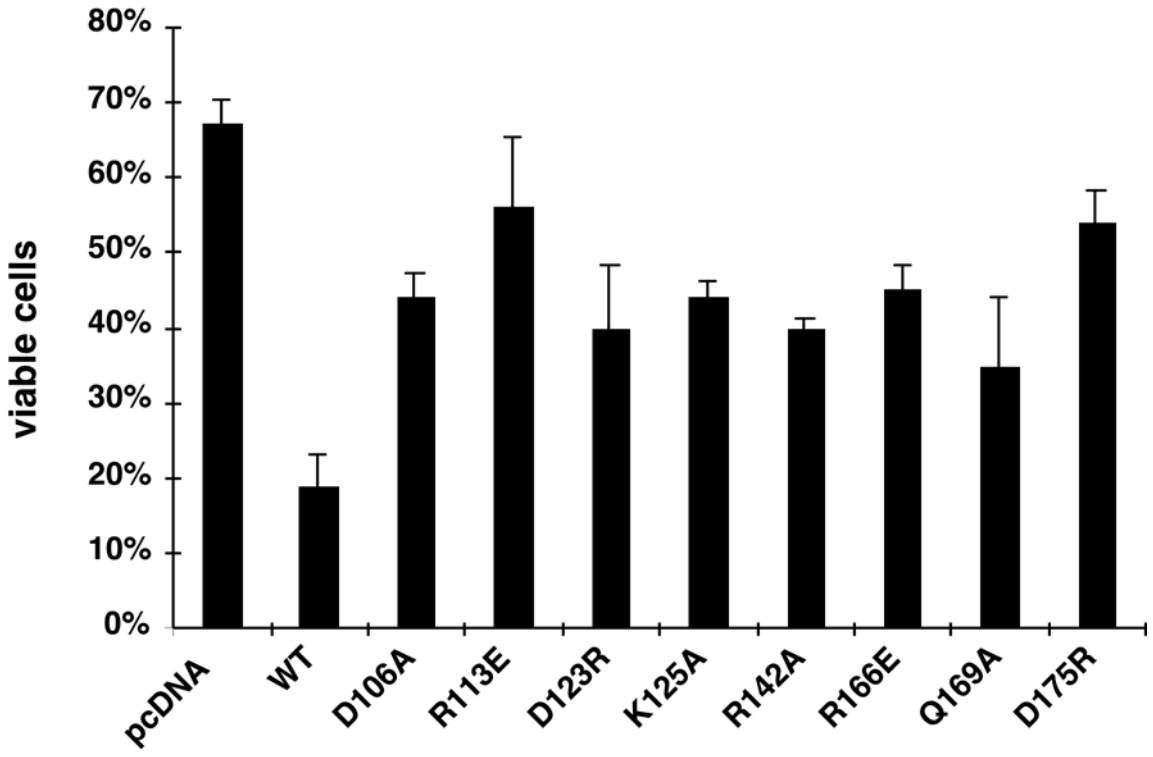
viable cells
80%
70%
60%
50%
40%
30%
20%
10%
0%
pcDNA
WT
D106A
R113E
D123R
K125A
R142A
R166E
Q169A
D175R

Figure A

Identification of an Expanded Binding Surface on the FADD Death Domain Responsible for Interaction with CD95/Fas

Justine M. Hill, Gaku Morisawa, Tad Kim, Ted Huang, Yu Wei, Yufeng Wei and Milton H. Werner

J. Biol. Chem. 2004, 279:1474-1481.
doi: 10.1074/jbc.M304996200 originally published online October 22, 2003
